Supplemental material for Probing the fluctuations of the optical properties in time-resolved spectroscopy

Francesco Randi,[1,2] Martina Esposito,[1] Francesca Giusti,[1] Oleg Misochko,[3,4] Fulvio Parmigiani,[1,5,6] Daniele Fausti,[1,5] and Martin Eckstein[2,7]

[1] *Department of Physics, Università degli Studi di Trieste, 34127 Trieste, Italy*
[2] *Max Planck Institute for the Structure and Dynamics of Matter, 22761 Hamburg, Germany*
[3] *Institute of Solid State Physics, Russian Academy of Sciences, Chernogolovka, Moscow Region 142432, Russia*
[4] *Institute of Nanotechnologies of Microelectronics, Russian Academy of Sciences, Moscow 119334, Russia*
[5] *Sincrotrone Trieste SCpA, 34127 Basovizza, Italy*
[6] *International Faculty, Universität zu Köln, 50937 Köln, Germany*
[7] *University of Hamburg-CFEL, 22761 Hamburg, Germany*

(Dated: September 6, 2017)

NONEQUILIBRIUM DMFT FOR THE HOLSTEIN MODEL

In this section we present the nonequilibrium DMFT setup for the Holstein model. Apart from the symmetry breaking, the formalism is analogous to what has been explained in Ref. [1]. We therefore only state the equations, and do not provide a detailed derivation.

In DMFT, the Holstein model [see Eq. (5) of the main text] is mapped to a set of Anderson-Holstein impurity models (one for each inequivalent lattice site), with action

$$\begin{aligned} S = &- i\sum_\sigma \int_C dt \left[\sqrt{2}gX\,(c^\dagger_\sigma c_\sigma - \tfrac{1}{2}) + \frac{\omega_0}{2}(X^2+P^2)\right] \\ &- i\sum_\sigma \int_C dt_1 dt_2\, c^\dagger_\sigma(t_1)\Delta(t_1,t_2)c_\sigma(t_2) \end{aligned} \tag{1}$$

on the Keldysh time-contour C. (For an introduction to nonequilibrium DMFT and to the Keldysh formalism, see Ref. [2]). In Eq. (1), the first term is the local part of the lattice Hamiltonian, which involves the coupling of the electrons at the impurity site to the coordinate $X = (b^\dagger + b)/\sqrt{2}$ of the local oscillator, and $\Delta(t_1,t_2)$ is the hybridization function, which is determined self-consistently below.

The impurity model is solved using the self-consistent Migdal approximation [1], where also the vibrational mode evolves as a consequence of the interaction with the electrons. In the symmetry broken phase, the coordinate X acquires a nonzero expectation value. The expectation value is determined by the exact equation of motion $\frac{d^2}{dt^2}\langle X(t)\rangle = -\omega_0^2\langle X(t)\rangle + F(t)$, with the time-dependent force $F(t)$

$$F(t) = \sqrt{2}g\sum_\sigma \big(\langle c^\dagger_\sigma(t)c_\sigma(t)\rangle - 0.5\big). \tag{2}$$

In turn, there is a time-local (Hartree) contribution to the electronic self-energy, i.e., a self-consistent on-site potential,

$$h_{loc}(t) = -\sqrt{2}g\langle X(t)\rangle. \tag{3}$$

Furthermore, we include the leading order self-consistent diagrammatic corrections in the expansion in terms of the fluctuations $\tilde{X} = X - \langle X(t)\rangle$. The second-order electronic self-energy is

$$\Sigma(t,t') = ig^2 G(t,t')D(t,t'), \tag{4}$$

where

$$D(t,t') = -2i\langle T_C \tilde{X}(t)\tilde{X}(t')\rangle. \tag{5}$$

(We consider the spin-symmetric phase and omit spin indices Σ_σ and G_σ.) With this, the Dyson equation for the electronic Green's function reads

$$\begin{aligned} &\big(i\partial_t + \mu - h_{loc}\big)G(t,t') - \\ &\qquad \big(\Delta(t,t') + \Sigma(t,t')\big) * G(t,t') = \delta_C(t,t'). \end{aligned} \tag{6}$$

To include the back-action of the electrons on the phonons on the same diagrammatic level, we include the phonon self-energy (polarization operator)

$$P(t,t') = -2ig^2 G(t,t')G(t',t), \tag{7}$$

and solve the phonon Dyson equation in the form

$$\big(1 - D_0(t,t') * P(t,t')\big) * D(t,t') = D_0(t,t'). \tag{8}$$

Here $D_0(t,t')$ is the non-interacting phonon propagator,

$$\begin{aligned} D_0(t,t') = &- i\big[2\cos(\omega_0(t-t')b_\beta + \theta_C(t',t)e^{i\omega_0(t-t')} \\ &+ \theta_C(t,t')e^{-i\omega_0(t-t')}\big], \end{aligned} \tag{9}$$

where $b_\beta = 1/(e^{\beta\omega_0}-1)$ is the Bose function.

In the present case of a two-sublattice symmetry broken phase, we have two inequivalent impurity models (1), which represent sites on the a and b sublattice, i.e., all quantities, G, Δ, h_{loc}, $\langle X(t)\rangle$, Σ, P, will additionally depend on the sublattice a, b. For the particle-hole symmetric case, we have $\langle X(t)\rangle_a = -\langle X(t)\rangle_b$. We use a bipartitle lattice with a semielliptic density of states, in which the DMFT self-consistency is given by [2]

$$\Delta_a(t,t') = v(t)G_b(t,t')v(t'), \tag{10}$$

$$\Delta_b(t,t') = v(t)G_a(t,t')v(t'), \tag{11}$$

where $v(t)$ is the time-dependent profile of the hopping amplitude. This closes DMFT equations.

Optical conductivity: The main quantity of interest in this work is the current correlation function $C(t,t') = \langle j(t)j(t')\rangle$, and the optical susceptibility $\delta\langle j(t)\rangle/A(t')$, which characterizes the long-wavelength current ($q \to 0$) in response to an applied time-dependent vector potential $A(t)$. Since the current operator is given by $j = -\delta H/\delta A$, the latter response function is given by $\chi^R(t,t') = i\theta(t,t')\langle[j(t), j(t')]\rangle$. (For simplicity of notation, we are omitting cartesian components x, y, z.)

The current-current correlation function is obtained from the lattice Green's function by direct generalization of the expressions presented in Ref. [3]. Both response and correlation function are obtained from the contour-ordered current-current correlation function,

$$\chi(t,t') = i\langle T_C j(t)j(t')\rangle. \tag{12}$$

which is defined as the response of the current to an arbitrary variation of the vector potential along the Keldysh contour,

$$\delta\langle j(t)\rangle = \int_C d\bar{t}\,\chi(t,\bar{t})\delta A(\bar{t}), \tag{13}$$

omitting a diamagnetic contribution which is time-local and thus irrelevant for the discussion of the dynamic properties discussed in this paper. Current fluctuations are given by the greater and lesser component, $\chi^>(t,t') \equiv \chi(t_-,t'_+) = i\langle j(t)j(t')\rangle$ and $\chi^<(t,t') \equiv \chi(t_+,t'_-) = i\langle j(t')j(t)\rangle$ ($t_\pm$ is on the upper/lower branch of the Keldysh contour), and $\chi^R(t,t') = \theta(t,t')(\chi^>(t,t') - \chi^<(t,t')$.

In the symmetry broken phase, the lattice has a unit cell with two sites a, b, and a reduced Brilluoin zone (RBZ). We introduce the spinor,

$$\hat{\psi}_k = \begin{pmatrix} c_{k,a} \\ c_{k,b} \end{pmatrix}, \tag{14}$$

and the momentum-dependent Green's function G_k then becomes a 2×2 matrix, $\hat{G}_k(t,t') = -i\langle T_C \hat{\psi}_k(t)\hat{\psi}_k^\dagger(t')\rangle$. The hopping term takes the form $H_{hop} = \sum_k \hat{\psi}_k^\dagger \epsilon_{k-A}\hat{\sigma}_1\hat{\psi}_k$, with the Pauli matrix $\hat{\sigma}_1$; $\sum_k$ is a sum over the reduced Brillouin zone (RBZ). The vector potential is added by the Peierls substitution $\epsilon_k \to \epsilon_{k-A}$, so that the current $j = -\delta H/\delta A$ is given by

$$\langle j(t)\rangle = -2i \sum_{k\in RBZ} \mathrm{tr}\big[v_{k-A}\hat{\sigma}_1\hat{G}_k(t_+,t_-)\big], \tag{15}$$

where $v_k = \partial_k\epsilon_k$ is the band velocity, and the factor 2 is for spin. Following Ref. [3], we take the variation $\delta A(t')$, using that vertex corrections to the current correlation function vanish in DMFT. This gives the susceptibility (evaluated at $A = 0$),

$$\chi(t,t') = 2i \sum_{k\in RBZ} v_k^2\,\mathrm{tr}\big[\hat{\sigma}_1\hat{G}_k(t_+,t')\hat{\sigma}_1 G_k(t',t_-)\big], \tag{16}$$

which is the usual bubble diagram of the Green's functions.

In DMFT (and when we consider only a modulation of the hopping amplitude, as in the manuscript), $\hat{G}_k$ depends on k only via the dispersion ϵ_k, i.e., $\hat{G}_k(t,t') \equiv \hat{G}_{\epsilon_k}(t,t')$. In the particle-hole symmetric case on a bipartite lattice, the RBZ corresponds to positive values of ϵ_k. The momentum sum can then be represented by integrals

$$\sum_{k\in RBZ} f(\epsilon_k) = \int_0^\infty \rho(\epsilon)f(\epsilon), \tag{17}$$

$$\sum_{k\in RBZ} v_k^2 f(\epsilon_k) = \int_0^\infty D(\epsilon)f(\epsilon), \tag{18}$$

where ρ and D depend on the lattice. We assume a semi-elliptic density of states $\rho(\epsilon) = \sqrt{4-\epsilon^2}$, and the corresponding form for $D(\epsilon)$ as defined in Ref. [3]. The lattice Green's function is evaluated on a grid of momentum points, solving the Dyson equation $\hat{G}_{\epsilon_k}(t,t') = (i\partial_t + \mu - \hat{h}(t) - \hat{\Sigma}(t,t'))^{-1}$, where $\hat{h}$ and $\hat{\Sigma}$ in the {a,b} basis are

$$\hat{h}(t) = \begin{pmatrix} gX_a(t) & \epsilon_k(t) \\ \epsilon_k(t) & gX_b(t) \end{pmatrix}, \tag{19}$$

$$\hat{\Sigma}(t,t') = \begin{pmatrix} \Sigma_a(t,t') & 0 \\ 0 & \Sigma_b(t,t') \end{pmatrix}, \tag{20}$$

with the sublattice-dependent $\Sigma_{a,b}$ and $\langle X\rangle_{a,b}$.

DERIVATION THE REFLECTIVITY FLUCTAUTIONS

In this section we present explicit steps of the fluctuation expansion leading from the general expression for the moments I_n of the photon-count [main text, Eq. (2)] to the variance of the intensity [main text, Eq. (1)]. We start from the expression for I_n,which was been derived by Fleischhauer [4, 5],

$$I_1 = \int d1d1'd\bar{1}d\bar{1}'\ \mathcal{D}_{11'}g(1,\bar{1})g(1',\bar{1}')\langle j(\bar{1})j(\bar{1}')\rangle, \tag{21}$$

$$I_2 = \int d1d1'd2d2'd\bar{1}d\bar{1}'d\bar{2}d\bar{2}'\ \mathcal{D}_{11'}\mathcal{D}_{22'}g(1,\bar{1})g(1',\bar{1}') \times\ g(2,\bar{2})g(2',\bar{2}')\langle T_{\bar{\tau}}[j(\bar{1})j(\bar{2})]T_\tau[j(\bar{1}')j(\bar{2}')]\rangle. \tag{22}$$

Here

$$\mathcal{D}_{1,1'} = \epsilon\delta(\boldsymbol{r}_1 - \boldsymbol{R})\delta(\boldsymbol{r}_1' - \boldsymbol{R})\int_0^\infty d\omega\, e^{-i\omega(t_1 - t_1')} \tag{23}$$

is the detector response function, and g is the linear kernel which relates the induced field E_{ind} and the current j by a solution of Maxwell equations,

$$E_{ind}(1) = \int d\bar{1}g(1,\bar{1})j(\bar{1}). \tag{24}$$

In Eq. (21) and (22), we insert the expansion $j(1) = \langle j(1)\rangle + \delta j(1)$. Terms which are first order in δj vanish by construction, because $\langle \delta j\rangle = 0$. Zeroth order terms are identical in I_2 and I_1^2, and thus vanish in the variance $I_2 - I_1^2$. Third and fourth order terms, such as Eq. (22) where the correlation function in the integrand is replaced by $\langle T_{\bar\tau}[\delta j(\bar 1)\delta j(\bar 2)]\delta j(\bar 1')\rangle\langle j(\bar 2')\rangle$, are not considered here as explained in the main text, because they scale differently with the sample volume. To second order in δj, Eq. (22) has six terms, where the current correlation function in the integral takes one of the following combinations

$$\begin{aligned}&\langle T_{\bar\tau}[\delta j(\bar 1)\delta j(\bar 2)]\rangle\langle j(\bar 1')\rangle\langle j(\bar 2')\rangle,\ \langle \delta j(\bar 1)\delta j(\bar 2')\rangle\langle j(\bar 1')\rangle\langle j(\bar 2)\rangle,\\ &\langle \delta j(\bar 2)\delta j(\bar 1')\rangle\langle j(\bar 1)\rangle\langle j(\bar 2')\rangle,\ \langle T_{\tau}[\delta j(\bar 1')\delta j(\bar 2')]\rangle\langle j(\bar 1)\rangle\langle j(\bar 2)\rangle,\\ &\langle \delta j(\bar 1)\delta j(\bar 1')\rangle\langle j(\bar 2)\rangle\langle j(\bar 2')\rangle,\ \langle \delta j(\bar 2)\delta j(\bar 2')\rangle\langle j(\bar 1)\rangle\langle j(\bar 1')\rangle.\end{aligned} \tag{25}$$

Here the time-ordering operator can be dropped whenever it acts on c-numbers $\langle j\rangle$, such as for the second term, $\langle T_{\bar\tau}[\delta j(\bar 1)\langle j(\bar 2)\rangle]T_\tau[\delta j(\bar 2')\langle j(\bar 1')\rangle]\rangle = \langle \delta j(\bar 1')\delta j(\bar 2)\rangle\langle j(\bar 1)\rangle\langle j(\bar 2')\rangle$. Of the six terms in Eq. (25), the last two are cancelled by corresponding terms in the expansion of I_1^2. For the remaining four, one can evaluate integrals in (22) which correspond to a contraction of the current expectation values $\langle j\rangle$ with $\mathcal{D}$,

$$\begin{aligned}&\int d\bar 1 d1\ \mathcal{D}_{1,1'} g(1,\bar 1)\langle j(\bar 1)\rangle\\ &= \epsilon\delta(\boldsymbol{r}_1' - \boldsymbol{R})\int d1\, E_{ind}(1)\,\delta(\boldsymbol{r}_1 - \boldsymbol{R})\int_0^\infty d\omega\, e^{-i\omega(t_1 - t_1')}\\ &= \delta(\boldsymbol{r}_1' - \boldsymbol{R})\int_0^\infty d\omega\, e^{-i\omega(t_1 - t_1')} E_{ind}(\boldsymbol{R}, t_1)\\ &\equiv \epsilon\delta(\boldsymbol{r}_1' - \boldsymbol{R})E_-(t_1'),\end{aligned} \tag{26}$$

using Eqs. (23) and (24) in the first step. Similarly,

$$\begin{aligned}&\int d\bar 1' d1'\ \mathcal{D}_{1,1'} g(1',\bar 1')\langle j(\bar 1')\rangle\\ &= \epsilon\delta(\boldsymbol{r}_1 - \boldsymbol{R})\int d1\, E_{ind}(1')\,\delta(\boldsymbol{r}_1' - \boldsymbol{R})\int_0^\infty d\omega\, e^{-i\omega(t_1 - t_1')}\\ &= \delta(\boldsymbol{r}_1 - \boldsymbol{R})\int_0^\infty d\omega\, e^{-i\omega(t_1 - t_1')} E_{ind}(\boldsymbol{R}, t_1')\\ &\equiv \epsilon\delta(\boldsymbol{r}_1 - \boldsymbol{R})E_+(t),\end{aligned} \tag{27}$$

Inserting Eqs. (25), (26), and (27) into Eqs. (22) and (21) we get

$$\begin{aligned}&I_2 - I_1^2 =\\ &=\epsilon^2\int d1d2d\bar 1 d\bar 2\, g(1,\bar 1)g(2,\bar 2)\ \times\\ &\quad\times\langle T_{\bar\tau}[\delta j(\bar 1)\delta j(\bar 2)]\rangle\delta(\boldsymbol{r}_1 - \boldsymbol{R})E_+(t_1)\delta(\boldsymbol{r}_2 - \boldsymbol{R})E_+(t_2)\\ &\quad+\epsilon^2\int d1d2'd\bar 1 d\bar 2'\, g(1,\bar 1)g(2',\bar 2')\ \times\\ &\quad\times\langle \delta j(\bar 1)\delta j(\bar 2')\rangle\delta(\boldsymbol{r}_1 - \boldsymbol{R})E_+(t_1)\delta(\boldsymbol{r}_2' - \boldsymbol{R})E_-(t_2')\\ &\quad+\epsilon^2\int d1'd2d\bar 1' d\bar 2\, g(1',\bar 1')g(2,\bar 2)\ \times\\ &\quad\times\langle \delta j(\bar 2)\delta j(\bar 1')\rangle\delta(\boldsymbol{r}_1' - \boldsymbol{R})E_-(t_1')\delta(\boldsymbol{r}_2 - \boldsymbol{R})E_+(t_2)\\ &\quad+\epsilon^2\int d1'd2'd\bar 1' d\bar 2'\, g(1',\bar 1')g(2',\bar 2')\ \times\\ &\quad\times\langle T_{\tau}[\delta j(\bar 1')\delta j(\bar 2')]\rangle\delta(\boldsymbol{r}_1' - \boldsymbol{R})E_-(t_1')\delta(\boldsymbol{r}_2' - \boldsymbol{R})E_-(t_2').\end{aligned}$$

$$\begin{aligned}&=\epsilon^2\int dt_1 dt_2\langle T_{\bar\tau}[\delta j(\boldsymbol{R},t_1)\delta j(\boldsymbol{R},t_2)]\rangle_{ret}E_+(t_1)E_+(t_2)\\ &\quad+\epsilon^2\int dt_1 dt_2'\langle \delta j(\boldsymbol{R},t_1)\delta j(\boldsymbol{R},t_2')\rangle_{ret}E_+(t_1)E_-(t_2')\\ &\quad+\epsilon^2\int dt_1' dt_2\langle \delta j(\boldsymbol{R},t_2)\delta j(\boldsymbol{R},t_1')\rangle_{ret}E_-(t_1')E_+(t_2)\\ &\quad+\epsilon^2\int dt_1' dt_2'\langle T_{\tau}[\delta j(\boldsymbol{R},t_1')\delta j(\boldsymbol{R},t_2')]\rangle_{ret}E_-(t_1')E_-(t_2').\\ &=2\epsilon^2\mathrm{Re}\int dt dt'\langle T_{\bar\tau}[\delta j(\boldsymbol{R},t)\delta j(\boldsymbol{R},t')]\rangle_{ret}E_+(t)E_+(t')\\ &\quad+2\epsilon^2\int dt dt'\langle \delta j(\boldsymbol{R},t)\delta j(\boldsymbol{R},t')\rangle_{ret}E_+(t)E_-(t').\end{aligned} \tag{28}$$

In the main text the first term is not discussed because it would vanish by averaging over a carrier envelope phase φ ($E_\pm \sim e^{\mp i\varphi}$). The remaining term is Eq. (1) of the main text.

ELECTRONIC OCCUPATION

To visualize more clearly how the electronic occupation and distribution function change during the oscillation, in Fig. 1a we plot the electronic occupation $N(t_p,\omega)$ and spectral function $A(t_p,\omega)$ for two pump-probe delays at the minimum and maximum of the oscillation of $\langle X\rangle$. Fig. 1b shows their ratio. As can be seen, when $\langle X\rangle$ is at its minimum and the atoms are the closest to the undistorted position, the distribution function closely resembles the Fermi-Dirac distribution. When $\langle X\rangle$ is maximum and the gap is revived after one period of the oscillation, the distribution function departs from the quasi-thermal thermal state.

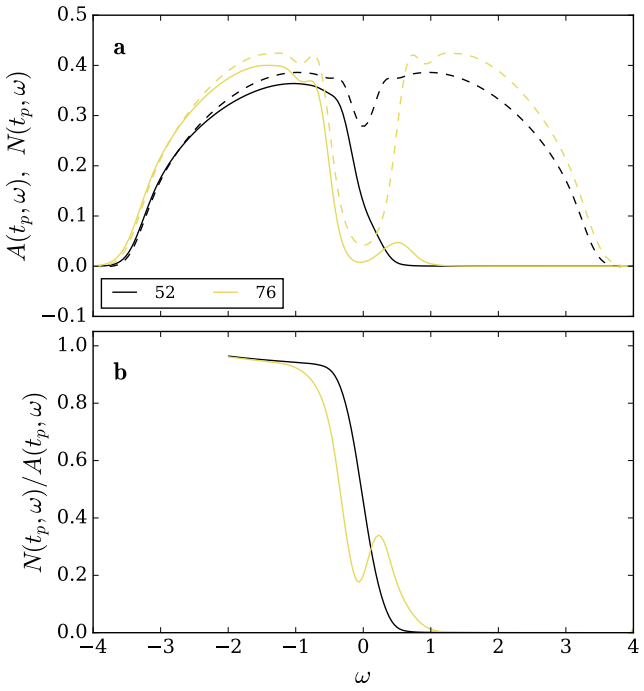

FIG. 1. **a)** Electronic occupation $N(t_p,\omega)$ (solid) and spectral function $A(t_p,\omega)$ (dashed) for pump-probe delays $t_p = 52, 76$ (black and yellow, respectively), i.e. at the minimum and maximum $\langle X\rangle$ in the oscillation. **b)** Ratio $N(t_p,\omega)/A(t_p,\omega)$ for the two t_p as in panel **a**.

EXPERIMENTAL SET-UP

The measurements reported in Fig. 3 of the main text have been performed with the set-up described by Esposito et al. [6]. In order to cancel classical fluctuations in the incoming light, a balanced differential detector has been used to measure $\frac{\Delta R}{R}$ and $(\Delta m)^2$. The probe beam is split in two. One of the resulting beams interacts with the sample, while the other is used as the reference for the balanced differential measurement. Due to extrinsic contributions to the noise in the measurement produced in the balanced scheme, the absolute amplitude of the modulation of the variance should not be considered as relevant.

Fig. 3 of the main text shows the total $(\Delta m)^2 = \sigma[I] + \langle m\rangle$, while Fig. 2b shows $C(t_p,\omega)$, which gives rise only to the contribution $\sigma_{\rm bulk}$ to $\sigma[I]$ (see Eq. 3 of the main text). They should be compared considering the fact that $(\Delta m)^2$ (Fig. 3) contains, in addition to $\sigma_{\rm bulk}$, a shot-noise-like term proportional to the probe pulse intensity and, hence, to $\frac{\Delta R}{R}$. The relevant information contained in Fig. 3 is the deviation of $(\Delta m)^2$ from the simple shot-noise-like behavior, i.e. from a rescaled $\frac{\Delta R}{R}$. Such deviation occurs, as predicted by the result of the numerical calculation (inset of Fig. 2b in the main text), after one period of the oscillation. Note that $\frac{\Delta R}{R} \propto -\langle X\rangle$.

[1] Y. Murakami, P. Werner, N. Tsuji, and H. Aoki "Interaction quench in the Holstein model: Thermalization crossover from electron- to phonon-dominated relaxation" Phys. Rev. B **91**, 045128 (2015).

[2] H. Aoki, N. Tsuji, M. Eckstein, M. Kollar, T. Oka, and P. Werner "Nonequilibrium dynamical mean-field theory and its applications" Rev. Mod. Phys. **86**, 779 (2014).

[3] M. Eckstein, and M. Kollar "Theory of time-resolved optical spectroscopy on correlated electron systems" Phys. Rev. B **78**, 205119 (2008).

[4] M. Fleischhauer, "Quantum-theory of photodetection without the rotating wave approximation", J. Phys. A: Math. Gen. **31**, 453 (1998).

[5] Note that we use a different notation with respect to Fleischhauer [4]. In particular, our kernel $g(1,2)$ corresponds to Fleischhauer's $D^{\rm ret}(1,2)$, our detector response $\mathcal{D}_{1,2}$ corresponds to Fleischhauer's $f(t_1,t_2)$, and our currents j are Fleischhauer's sources s.

[6] M. Esposito, K. Titimbo, K. Zimmermann, F. Giusti, F. Randi, D. Boschetto, F. Parmigiani, R. Floreanini, F. Benatti, and D. Fausti, "Photon number statistics uncover the fluctuations in non-equilibrium lattice dynamics", Nat. Comm. **6**, 10249 (2015).